Available online at www.sciencedirect.com
SCIENCE DIRECT®
Chemical Physics Letters 397 (2004) 296–301
CHEMICAL PHYSICS LETTERS
www.elsevier.com/locate/cplett

Optical characterization of DNA-wrapped carbon nanotube hybrids

S.G. Chou [a,*], H.B. Ribeiro [b], E.B. Barros [c,d], A.P. Santos [e], D. Nezich [f], Ge.G. Samsonidze [d], C. Fantini [b], M.A. Pimenta [b], A. Jorio [b], F. Plentz Filho [b], M.S. Dresselhaus [d,f], G. Dresselhaus [g], R. Saito [h], M. Zheng [i], G.B. Onoa [i], E.D. Semke [i], A.K. Swan [j], M.S. Ünlü [j], B.B. Goldberg [j,k]

[a] *Department of Chemistry, Massachusetts Institute of Technology, 13-3029, #77 Massachusetts Ave., Cambridge, MA 02139-4307, USA*
[b] *Depto. de Física, Universidade Federal de Minas Gerais, Belo Horizonte-MG 30123-970, Brazil*
[c] *Departamento de Física, Universidade Federal do Ceará, Fortaleza-CE 60455-760, Brazil*
[d] *Department of Electrical Engineering and Computer Science, Massachusetts Institute of Technology, Cambridge, MA 02139-4307, USA*
[e] *Centro de Desenvolvimento da Tecnologia Nuclear, CDTN/CNEN, Belo Horizonte-MG 30123-970, Brazil*
[f] *Department of Physics, Massachusetts Institute of Technology, Cambridge, MA 02139-4307, USA*
[g] *Francis Bitter Magnet Laboratory, Massachusetts Institute of Technology, Cambridge, MA 02139-4307, USA*
[h] *Department of Physics, Tohoku University and CREST JST, Sendai 980-8578, Japan*
[i] *DuPont Central Research and Development, Experimental Station, Wilmington, DE 19880-0356, USA*
[j] *Electrical and Computer Engineering Department, Boston University, Boston, MA 02215-1714, USA*
[k] *Department of Physics, Boston University, Boston, MA 02215-1714, USA*

Received 14 July 2004; in final form 14 July 2004
Available online 16 September 2004

Abstract

Optical characterization of DNA-wrapped CoMoCAT carbon nanotube hybrids (DNA–CNT) and semiconductor-enriched DNA–CNT was carried out using resonant Raman spectroscopy (RRS) and photoluminescence (PL) experiments. The values of radial breathing modes frequency ω_{RBM} were found to be relatively insensitive to the type of wrapping agents surrounding the nanotube. The values of ω_{RBM} and the first and second resonant interband transitions, E_{11} and E_{22}, for a particular (n,m) tube for all sample types in RRS and PL measurements are found to correspond to the values obtained for SDS-dispersed nanotubes measured with PL, but with a shift in E_{ii} ranging from 10 to 80 meV. The DNA-wrapping has shown not only to provide good isolation to the individual nanotube in a bundle, but the DNA wrapping mechanism for the CoMoCAT sample has also been shown to be diameter selective.

1. Introduction

As the nature of materials research becomes increasingly interdisciplinary, numerous long-standing research problems have been revisited in recent years using biological methods for materials modification. One of the most exciting applications of such biological methods is the separation of single wall nanotubes (SWNTs) using single stranded DNA (ss-DNA) to modify the interaction between a carbon nanotube (CNT) and its environment [1,2].

Previous studies [1,2] have shown that ss-DNA of the poly-d(GT) sequence forms a stable complex with individual SWNTs by wrapping around them via the aromatic interactions between the guanine (G) and thymine (T) bases and the nanotube sidewall. By passing such hybrids through an ion exchange chromatography (IEC) column, fractions strongly enriched with CNTs of specific metallicities and with a modified diameter distribution can be obtained [2,3].

* Corresponding author.
E-mail address: grace@mgm.mit.edu (S.G. Chou).

0009-2614/$ - see front matter © 2004 Elsevier B.V. All rights reserved.
doi:10.1016/j.cplett.2004.08.117

The IEC separation of DNA–CNT hybrids has received considerable attention recently, and various aspects of this separation have been investigated [3,4]. However, relatively little is known about how the physical properties of the nanotubes are affected by the different degrees of isolation achieved using different wrapping agents.

In this work, a resonant Raman spectroscopy (RRS) study was carried out on DNA–CNT hybrids to investigate the effects of DNA and CNT interactions. A semiconductor-enriched (S-enriched) fraction of DNA–CNT hybrids from an IEC separation (fractionation) was studied to understand the effect of the S-enrichment. The Raman measurements show that the DNA wrapping is a diameter selective process for the CoMoCAT nanotubes, and the fractionation procedure further decreases the metallic components of the sample, as shown previously for the case of HiPco SWNTs [5]. Photoluminescence (PL) mapping was carried out to study the PL process in the DNA–CNT hybrid system. Electronic transitions, E_{ii}, were observed over a wide range of excitation energies, E_{laser}, for both samples. The values of the radial breathing mode frequencies, ω_{RBM}, and of the interband transition energies E_{ii} of the DNA–CNT hybrids measured by RRS and PL experiments can be well-correlated with the previously established ($2n + m$ = constant) family patterns for SDS-encapsulated HiPco nanotubes [5].

2. Experimental

Thirteen laser excitation energies, E_{laser}, were used in the RRS measurements, including the 2.71 eV (458 nm), 2.60 eV (477 nm), 2.54 eV (488 nm), 2.50 eV (497 nm), 2.47 eV (502 nm), 2.41 eV (514 nm), 2.18 eV (568 nm) and 1.92 eV (647 nm) lines from an Ar/Kr laser; 1.97 eV (633 nm), 1.94 eV (640 nm) and 1.88 eV (658 nm) from a dye laser (using DCM dye), pumped by an Ar^+ ion laser; 1.97 eV (633 nm) from a HeNe laser; and 2.33 eV (532 nm) from a Nd:YAG/Nd:YVO4 crystal laser. A Dilor XY triple monochromator spectrometer was used in conjunction with the Ar/Kr and the dye laser, wheras an air-cooled CCD detector attached to a Renishaw 1000B micro-Raman system was used in conjunction with the 1.96 and 2.33 eV excitation. All scattered light was collected through a 50× microscope objective in the backscattering geometry. The laser power level was kept below 0.5 mW to prevent overheating the sample, and the average temperature (T) of the DNA–CNT sample was ~350 K [6].

Although a small degree of heating (~50 K), was observed, previous studies [7,8] showed that, the 50 K increase in T should not shift the RBM frequencies by more than 1 cm^{-1}, and the changes in spectral intensities do not shift the E_{22}^{S} value by more than 2 meV, which is smaller than the uncertainty in the experimental E_{ii} determination (5 meV) [9].

SWNTs produced using CoMoCAT catalysts [10,11], which yield SWNTs with a narrow diameter (d_t) and chiral angle (θ) distribution, were used as the starting material, following previously described procedures [1,2]. CoMoCAT-based DNA–CNT samples were analyzed by RRS (on dried SWNT bundles and DNA–CNT hybrids) and by PL (on DNA–CNT hybrids in solution) experiments.

The dried DNA–CNT samples were prepared by dropping 30 μL of the stock solution onto a sapphire substrate 1 μL at a time. The drops were allowed to dry into a thick layer of nanotubes. An as-produced, CoMoCAT-based, non-fractionated DNA–CNT sample and an S-enriched DNA–CNT sample obtained from the IEC fractionation process [2] were all studied. Optical absorption studies [12] have shown that the fractionated sample is strongly enriched in (6, 5) SWNTs.

The PL experiments were carried out in a DNA–CNT hybrid solution diluted 20 times from a stock solution. The samples were then placed in a glass cuvette with an optical beam path of 1mm. The sample was excited using a tunable Ti:Sapphire laser, which is pumped by a high power Ar^+ ion laser. The emitted light was collected in a back scattering geometry and was focused onto a North Coast Ge detection system and a Spex 750M Spectrometer.

3. Results and discussion

3.1. E_{22}^S measurements from the anti-Stokes and Stokes RRS experiments

Stokes and anti-Stokes RRS measurements were carried out on DNA–CNT hybrid samples. In most non-resonant Raman scattering events, the relative spectral intensities for the Stokes and anti-Stokes processes reflect the temperature dependence of the relative phonon populations. In nanotube systems where the joint density of states (JDOS) has sharp van Hove singularities, the anti-Stokes/Stokes intensity ratio ($I_{\text{AS}}/I_{\text{S}}$) is dominated by the resonance process. Values of E_{ii} were determined from the intersection of the resonance windows for the AS and S scattering processes [13]. The widths of the resonance window profiles are denoted by the parameter, Γ_{r}, in the spectral intensity equation [13], and Γ_{r} gives information about the excited state relaxation rate and the inhomogeneous broadening of the resonance window. The intensity ratios of the resonance window profiles, constructed using the average Γ_{r} values for each type of sample with similar wrapping agents [14], were compared to the ratios of the temperature-normalized $I_{\text{AS}}/I_{\text{S}}$ ratios at E_{laser} to obtain an experimental determination of E_{ii} [13,15].

The resonance windows for the dried unfractionated DNA–CNT hybrids have an average Γ_r value of 15 meV, which is narrow compared to the Γ_r for pristine (not wrapped) CoMoCAT nanotubes in bundles (100 meV) and the Γ_r for SDS-dispersed HiPco nanotubes in solution (60 meV) [9]. Without the inhomogeneous broadening effects arising from the helical DNA-wrapping, the Γ_r value for an isolated nanotube on a SiO_2 substrate [16] has been found to be less than 10 meV. The relatively narrow resonance window for DNA–CNT CoMoCAT hybrids determined here suggests that although a large number of nanotubes were measured under the laser light spot in the dried DNA–CNT hybrid sample, the individual nanotubes in the DNA–CNT hybrid bundles were well isolated from one another and were only slightly affected by inhomogeneous broadening effects associated with nanotube bundling. With a smaller proportion of metallic (M) SWNTs present, the fractionated, semiconductor (S)-enriched DNA–CNT sample had a slightly smaller Γ_r (by less than ~1.5 meV) than that of the non-fractionated DNA–CNT sample.

To facilitate comparison with the work of others, the RRS-determined E_{22}^S values for S SWNTs were plotted against the radial breathing mode frequencies, ω_{RBM}, in Fig. 1. The colored square data points denote the two DNA-wrapped SWNT samples with different S to M ratios. To help with the interpretation of the RRS data, the RRS-measured E_{22}^S values for the DNA–CNT hybrids are compared to the E_{22}^S values measured using the PL technique for an SDS dispersed HiPco nanotube sample in solution, for which a previously

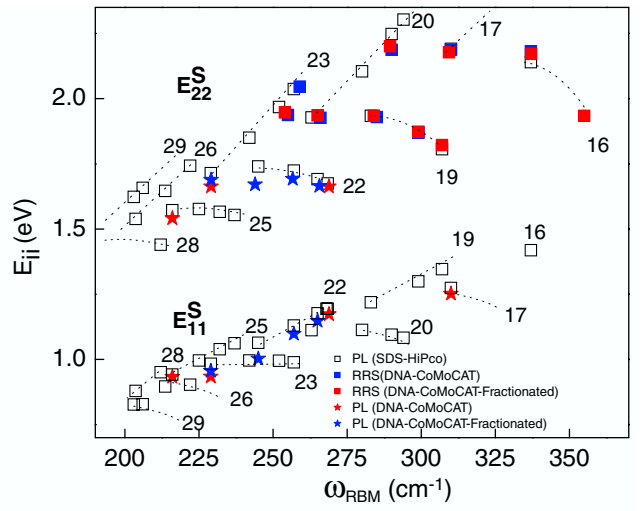

Fig. 1. E_{22}^S determined from the temperature-normalized I_{AS}/I_S ratios of the RRS spectra, plotted against ω_{RBM}, showing the ($2n + m$ = constant) family behavior. Colored data points denote the two DNA-wrapped samples with different S:M ratios (see text), measured with both RRS and PL. (For interpretation of the references to color in this figure legend, the reader is referred to the web version of this article.)

determined fitting formula was employed to extract the corresponding ω_{RBM} values [5,17]. The RRS measured ω_{RBM} values for the DNA–CNT hybrids in the present work correspond very well with the formula-extracted ω_{RBM} for the SDS nanotubes with the same (n,m) assignment [5]. From the comparison of E_{22}^S vs. ω_{RBM} values, the DNA–CNT hybrids were found to follow the ($2n + m$ = constant) family patterns previously determined from PL measurements of SDS-encapsulated samples [5]. SWNTs in the same family are connected by the dotted lines in Fig. 1, and the family numbers are shown. The wrapping of DNA was found to shift the second interband transition, E_{22}^S, by 10–80 meV, relative to SDS-isolated HiPco nanotubes with the same (n,m) assignment. Fractionated and non-fractionated samples were found to be shifted by different amounts, in the same direction, either blue or red shifted relative to SDS-encapsulated nanotubes. The average shift over all of the nanotubes measured comes out to be about 30 meV to the red. Since the SDS-encapsulated HiPco nanotubes were in solution, whereas the DNA-wrapped nanotubes are dried, the difference in environment could possibly contribute to the difference in the E_{22} transition energies.

Even though good agreement can be obtained between the ω_{RBM} and E_{22}^S values of SWNTs wrapped in different agents, as shown above, analysis of other phonon features shows that environmental effects play an important role in CNT optical processes. Effects of DNA-wrapping and solvation were also observed in the changes in other Raman modes of the various samples studied in the present work, as discussed below.

Fig. 2a shows the changes in the RBM spectra at different laser excitation energies. The differences between the RBM spectra between pristine, unwrapped nanotubes and the DNA-wrapped nanotubes indicate that the wrapping mechanism is diameter-selective, selecting nanotubes within a specific diameter range that fits the specific dimensions of the GT-DNA. As shown in Fig. 2a, the intensity of the RBM for smaller and larger diameter tubes outside of the range of 240–320 cm^{-1} are largely reduced or eliminated as the GT-DNA strands wrap around the nanotubes. The mechanism for DNA-assisted separation of HiPco CNTs using IEC has been discussed in detail in previous works [1,2]. The diameter selectivity is evident in the case of DNA-wrapped CoMoCAT nanotubes, as a result of the smaller and narrower diameter distribution of the CoMoCAT nanotubes. The separation of nanotubes by diameter and metallicity can be further achieved by sending the DNA-wrapped starting material through IEC fractionation columns.

The environmental effects of DNA-wrapping and the effects of the different ratios of S to M nanotubes within the sample are shown in the G-band spectra of Fig. 2. Fig. 2b shows a comparison of the G-band spectra of

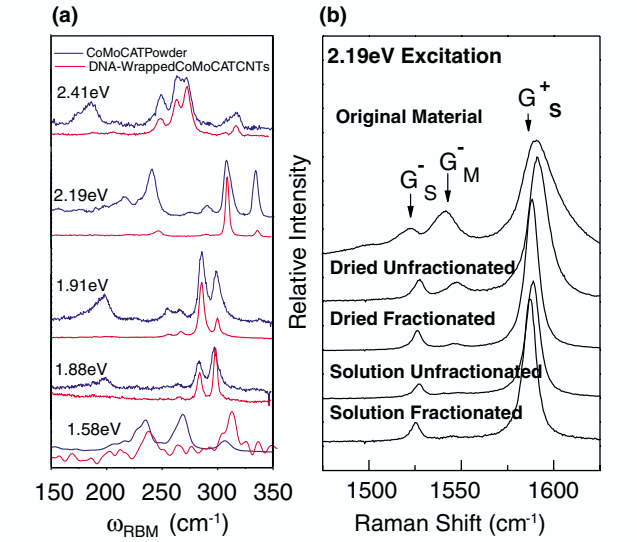

Fig. 2. (a) A comparison of RBM spectra of CoMoCAT bundles and DNA-wrapped CoMoCAT CNTs taken at different laser excitation energies (see text). (b) A comparison of the G-band spectra of different CoMoCAT-based DNA–CNT samples taken with 2.19 eV laser excitation (see text). After the bundles are broken up by DNA-wrapping, the different species within the bundle only interact weakly.

different environments taken at $E_{\text{laser}} = 2.19$ eV. Since previous PL experiments [10,18] showed that 2.19 eV excitation is strongly in resonance with the E_{22}^{S} transition of the (6, 5) nanotube, the G-band Raman spectra in Fig. 2b are dominated by the resonant transitions of the (6, 5) nanotubes, as indicated by the dominant RBM peak at 310 cm^{-1}. Progressively narrower linewidths of the various G-band components are seen in Fig. 2b as the intertube interactions are first reduced by DNA-isolation, then as the DNA–CNT sample becomes S-enriched, and finally as the DNA-hybrids are separated from one another by solvation, reflecting the progressively more homogeneous environment of the (6, 5) SWNTs. This observation is consistent with the decreasing Γ_r values as the nanotube is wrapped with a ss-DNA strand, and as the sample becomes S-enriched, as mentioned above.

DNA-wrapping and fractionation also affect the intensity and frequencies of the various G-band components. Five components were observed in the G-band spectra of the CoMoCAT starting material in Fig. 2b. The peak at 1590 cm^{-1} can be associated with the diameter-independent G^+ component with A/E_1 symmetry, whereas the peaks at 1541 and 1526 cm^{-1} can, respectively, be associated with the diameter-dependent G^- component for the larger diameter M CNTs (G_M^-) and the smaller diameter S CNTs (G_S^-) of either A or E_1 symmetry [19]. In addition, two smaller intensity peaks identified with E_2 symmetry were observed at 1498 and 1604 cm^{-1}.

Relative G_M^- intensity decreases are observed as more small diameter (*S*) CNTs are selected by DNA-wrapping. The intensity of the G_M^- further decreases as the number of M CNT decreases in the fractionated sample. As the samples were wrapped by DNA, the E_2 modes disappeared, suggesting that the isolation achieved by DNA-wrapping quenches such E_2-type transitions in nanotubes.

For an excitation energy at 2.19 eV shown in Fig. 2b, a consistent upshift in all the G^- peak frequencies of about 6 cm^{-1}, as well as a small downshift of 2 cm^{-1} in the G^+ peak frequency, relative to the CoMoCAT starting material, were observed for all DNA-wrapped samples. The G^- upshift could be identified with the changes in the in-plane vibrational force constant, resulting from the DNA–CNT interactions. An average downshift of the G^+ feature for dried and solution DNA-wrapped SWNTs samples is found to be about 2 cm^{-1}. This can be attributed to the combination of a small degree of perturbed in-plane vibrations and the charge transfer between the electron-donating species of DNA molecules and SWNTs. For most laser excitation energies, the magnitude of this charge transfer effect is found to be slightly larger when the samples are in solution.

3.2. Photoluminescence measurements

PL measurements were carried out to investigate the effect of fractionation and DNA-wrapping. From PL measurements over a wide range of excitation energies, the E_{11}^{S} and E_{22}^{S} transitions of the DNA–CNT hybrids were determined. Fig. 3 shows a section of the two-dimensional contour plot of the excitation

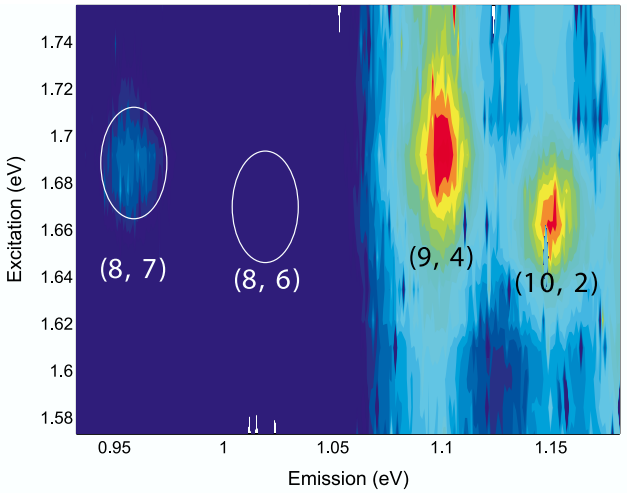

Fig. 3. A slice of the 2D contour plot of excitation vs. emission energies for a section of the PL data for the unfractionated DNA–CNT sample where $E_{22}^{S} \rightarrow E_{11}^{S}$ absorption–emission transitions are found. The (n, m) assignments for these transitions can be identified by comparing their energies with the assigned PL transitions for SDS-dispersed HiPco SWNTs [5]. Note that the (8, 6) transition is denoted by the white ellipse. The intensity of the transition is too weak to show up on the scale of the present plot.

vs. emission energies for the unfractionated sample in solution in the near-IR region. PL signals were observed from both fractionated and non-fractionated samples.

The energy positions for all of the E_{22} and E_{11} transitions measured for the two samples using Raman and PL are listed in Table 1. The excitation and emission energies for these peaks can be correlated with the E_{22}^{S} and E_{11}^{S} energies previously measured for SDS-encapsulated HiPco nanotubes in solution, as shown in Fig. 1. The average width of these absorption bands is ~30 meV for both the SDS/HiPco and DNA/CoMoCAT tubes.

Fig. 1 shows the energies of the E_{22} and E_{11} emission peaks for the DNA–CNT hybrids, together with previously reported values for SDS-dispersed nanotubes [5,17] and the E_{22} values measured with RRS. Even though most of the E_{ii}^{S} values captured in our PL experiments appear to be red-shifted from the values previously reported for SDS-encapsulated SWNTs with the same (n,m) assignments (see Table 1), these previously reported values can be used as a guide for us to draw similar ($2n + m$ = constant) family patterns for the PL peaks of DNA–CNT samples. Even though absorption could occur over a relatively broad range of E_{22}^{S} excitation energies, the E_{11}^{S} emission energy is clearly associated with the transition occurring at the band edge. Since the emission profile is relatively sharper, the uncertainties in the measured E_{11}^{S} values are expected to be smaller [18].

Compared to the values of E_{ii} obtained for SDS-isolated HiPco nanotubes with the same (n,m) assignment, most of the PL-determined shifts in the E_{22}^{S} and E_{11}^{S} values for DNA–CNTs are found to be less than 30 meV, which is consistent with the shifts observed in the E_{22}^{S} values measured using RRS, as mentioned above (see Table 1). The shifts in E_{ii} values between the SDS and DNA wrapped nanotubes measured both in RRS and PL suggest that the electronic structures of the nanotubes are perturbed differently by different wrapping agents and by different nanotube environments. In addition, the difference in E_{ii} between the fractionated and unfractionated samples suggests that even though the DNA effectively isolates the nanotubes from its environment, the homogeneity of the sample makes a difference in the electronic structure of individual SWNTs.

PL peaks for (9,7) and (11,0) SWNTs are found in the contour plot for the fractionated sample, while the transitions for the corresponding nanotubes do not appear in the PL spectra for the non-fractionated DNA–CNT hybrids. This suggests that the fractionation process eliminated some of the brightly luminescing species and brought out the transitions associated with species that were present in the original sample in small quantities and were too weak to be seen before. A 30 meV red shift was observed for the (8,7) nanotube in the fractionated sample, relative to its non-fractionated counterpart. This suggests that even though the DNA-wrapping has increased the physical distance between different nanotubes, the interactions between different species in the non-fractionated sample reduced the homogeneity of the environment, perturbed the nanotube electronic structure, and changed the E_{ii} by a small amount. Similar shifts in the E_{ii} values for nanotubes of the same (n,m) assignments between the dried fractionated and dried non-fractionated sample were also observed in the RRS E_{ii} determination, as shown in Fig. 1.

Table 1
Transition energies of DNA–CNT hybrids compared to SDS-encapsulated CNTs measured in PL experiments

(n,m)	d_t	DNA–CNT hybrids		Frac. DNA–CNT hybrids		SDS-wrapped CNTs [5]	
		E_{22}^{S} (eV)	E_{11}^{S} (eV)	E_{22}^{S} (eV)	E_{11}^{S} (eV)	E_{22}^{S} (eV)	E_{11}^{S} (eV)
(9,7)	1.103			1.541(PL)	0.933(PL)	1.572	0.942
(8,7)	1.018	1.689(PL)	0.956(PL)	1.663(PL)	0.934(PL)	1.714	0.983
(8,6)	0.953	1.671(PL)	1.003(PL)			1.740	1.064
(10,3)	0.923	1.938(RRS)		2.046(RRS)		1.959	
(9,4)	0.903	1.692(PL)	1.102(PL)			1.724	1.130
(11,1)	0.903	2.046(RRS)				2.029	
(7,6)	0.883	1.927(RRS)		1.936(RRS)		1.916	
(10,2)	0.872	1.665(PL)	1.190(PL)			1.691	1.177
(11,0)	0.862			1.663(PL)	1.176(PL)	1.675	1.194
(7,5)	0.818	1.930(RRS)		1.935(RRS)		1.925	
(9,2)	0.795	2.188(RRS)		2.201(RRS)		2.251	
(8,3)	0.771	1.869(RRS)		1.873(RRS)		1.870	
(6,5)	0.747	2.186(RRS)	1.257(PL)	2.186(RRS)	1.252(PL)	2.191	1.274
(9,1)	0.747			1.822(RRS)		1.789	
(6,4)	0.684			2.181(RRS)		2.140	
(7,2)	0.641			1.934(RRS)		1.981	
(5,4)	0.612			2.502(RRS)		2.567	

4. Conclusions

In this study, different samples of CoMoCAT CNT-based DNA-DNT hybrids were studied with RRS and PL experiments. DNA-wrapping and fractionation provide new means for probing the electronic structure of the nanotube 1D electronic structure by isolating the individual nanotubes from inter-tube interactions and by removing most of the metallic nanotubes to create a more homogeneous nanotube environment, thereby increasing the excited state lifetimes for PL. By monitoring the changes in the phonon spectra, the DNA-wrapping of CoMoCAT samples was found to be the diameter-selective aspect of DNA-wrapping. Also, the effects of fractionation were characterized. The good isolation achieved by DNA-wrapping and by the removal of metallic nanotubes through fractionation also brings out well-defined components of the G-band features, and suppresses the E_2-type phonon transitions. The RBM frequencies are found to be relatively insensitive to the nanotube environment. Through monitoring the shifts in the interband transition energies for DNA–CNTs, relative to SDS-encapsulated nanotubes and fractionated, S-enriched DNA–CNT samples, using RRS and PL, the environmental effects are found to play a small but non-negligible role regarding the E_{ii} determination. The electronic structure of nanotubes can be perturbed differently when the tubes are situated in different environments, and the E_{ii} can change by different amounts.

Acknowledgements

The experimental work was performed at the micro-Raman laboratory and semiconductor optics laboratory, Universidade Federal de Minas Gerais, Brazil, and was supported by FAPEMIG, CNPq and FINEP. The MIT authors acknowledge support under the Dupont-MIT Alliance and under NSF Grants DMR 01-16042 and INT 00-00408. R.S. acknowledges a Grant-in-Aid (Nos. 13440091 and 16076201) from Ministry of Education, Japan. Part of the experimental work was performed at the Boston University Photonics Center, operated in conjunction with their Department of Physics and the Department of Electrical and Computer Engineering. E.B. Barros acknowledges support from CAPES. The BU authors acknowledge support from NSF NIRT ECS-0210752. The Brazilian authors acknowledge support from the Instituto de Nanosciencias, Brazil.

References

[1] M. Zheng et al., Nat. Mater. 2 (2003) 338.
[2] M. Zheng et al., Science 302 (2003) 1545.
[3] V.W. Brar et al., J. Nanosci. Nanotech. 2004, in press.
[4] M.S. Strano, Nano Lett. 4 (2004) 543.
[5] M.S. Strano, J. Am. Chem. Soc. 125 (2003) 16148.
[6] By monitoring the changes in the normalized anti-Stokes to Stokes intensity ratios at different power levels between 0.050 and 0.49 mW, the average temperature of the DNA–CNT sample was extrapolated to be ~350 K.
[7] N.R. Raravikar et al., Phys. Rev. B 66 (2003) 235424(1).
[8] S. Chiashi, Y. Murakami, Y. Miyauchi, S. Maruyama, Chem. Phys. Lett. 386 (2004) 89.
[9] C. Fantini et al., Phys. Rev. Lett. 2004, in press.
[10] S.M. Bachilo et al., J. Am. Chem. Soc. 125 (2003) 11186.
[11] D. Resasco et al., J. Nano. Res. 4 (2002) 131.
[12] M. Zheng, Private communication.
[13] A.G. Souza Filho et al., Phys. Rev. B 63 (2001) 241404R.
[14] The Γ_r for each sample was empirically determined for each RBM feature by plotting the Raman peak intensities versus E_{laser} for a few closely spaced E_{laser} values, and then using a least squares fit routine to determine the widths and peak values of each intensity profile. The values of Γ_r for dried DNA-wrapped nanotubes and for as-produced CoMoCAT SWNT bundles were experimentally determined, respectively, by averaging over data acquired for five dried S DNA-wrapped nanotubes and for three S as-produced CoMoCAT nanotubes in a bundle.
[15] A.G. Souza Filho et al., Phys. Rev. B 69 (2004) 115400.
[16] A. Jorio et al., Phys. Rev. B 63 (2001) 245416.
[17] M.J. O'Connell et al., Science 297 (2002) 593.
[18] Y. Miyauchi, S. Chiashi, Y. Murakami, Y. Hayashida, S. Maruyama, Chem. Phys. Lett. 387 (2004) 198.
[19] G_M^- is generally associated with a broad, asymmetric spectral profile due to phonon–plasmon interactions. However, the plasmon interactions were suppressed in this case, and the G_M^- feature could be fitted with a Lorentzian.